

Experimental and numerical study of a broad pass-band low-loss optical metamaterials filter



Min Zhong*

Hezhou University, Hezhou, Guangxi 542899, China
Department of Physics, Nanjing Normal University, Nanjing 210023, China

ARTICLE INFO

Article history:

Received 16 March 2015
Received in revised form 24 June 2015
Accepted 25 June 2015
Available online 6 July 2015

OCIS:

160.3918
160.4236
260.1180
260.3910
160.5298

Keywords:

Metamaterials
Pass-band
Localized surface plasmon
Filter
Impedance matched

ABSTRACT

We present the simulation, and fabrication of an optical metamaterial filter. It consists of two silver layers and one SU-8 layer perforated with periodic sub-wavelength holes arrays which are prepared by optical lithography. Measured results indicate that a broad pass-band with over 96% transmittance across 90.0–105.0 THz frequency range can be obtained. Effective permeability, permittivity, and impedance are retrieved by applying *S* parameter retrieval method. These retrieved effective parameters show that the fabricated metamaterial filter can be modulated from a double negative material to a normal material in pass-band. Real parts of effective permeability and permittivity follow a similar slope results in well-matched impedance to free space, which leads to the broad pass-band. Furthermore, effects of nano-hole sidewall length (w_2) and thickness of dielectric layer (h_1) are experimental surveyed. The pass-band is expanded with w_2 increasing or h_1 reducing due to the reduced of strength of electromagnetic resonance.

© 2015 Elsevier B.V. All rights reserved.

1. Introduction

Properties of optical metamaterials composed of optically thick metallic films have been theoretically explained and experimentally verified by several investigators [1–4]. These properties would be applied to either significantly improve the performance of the existing optical devices or to develop entirely new optical devices, such as perfect absorber, superlens, and optical clock [5–8]. There is an increasing demand for the design of a broad pass-band optical metamaterial filter to make ensuring multi-frequency operations and high tolerance to the manufacture parameters. Naturally, properties of optical metamaterials filter are relied on the specific geometry arrangement of the unit cell [9], which would lead to strong dispersive behaviors across resonant band. Moreover, such a strong dispersive band usually contains interesting index regions, such as negative or zero/low index values (effective refractive index, permittivity, and permeability). These dispersive behaviors will limit the application of optical

metamaterial filter [10–12]. To avoid these dispersive behaviors, one of the design principles is to use multiple stacked metallic layers to obtain a pass-band. However, this design principle is complicate and difficult to be applied at the optical frequency. The electromagnetic resonance responses need to be carefully controlled across the pass-band, which results in the geometric parameters arrangements more complex. An alternative method is to design the structure which operates at frequency far away from the resonant band to avoid these strong dispersion behaviors [13,14]. Some literatures propose that the dispersive band can be exploited to meet the specific optical device needs and exploit new optical function [15–17]. Therefore, it is interesting to design a composite structure metamaterial filter by tailoring these dispersive behaviors for broad pass-band and low loss optical functions. In this paper, we propose a modified fishnet structure to modulate these dispersive behaviors in the pass-band. Measured results indicate that a broad pass-band optical metamaterial filter can be achieved with over 96% transmittance from 90.0 to 105.0 THz. The effective impedance is well-matched to the free-space throughout the whole pass-band. Such a metamaterial filter can provide an approach to select the targeted frequency band and thus leads to useful practical applications.

* Address: Hezhou University, Hezhou, Guangxi 542899, China.
E-mail address: zhongmin2012hy@163.com

2. Simulation methods and experimental details

Finite-element numerical simulations are performed with commercial Ansoft's HFSS 13.0. To achieve a broad pass-band, two air nano-holes are "added" on each corner of traditional fishnet structure, as shown in Fig. 1. The intermediate dielectric layer is SU-8 [18]. Such a compound structure may achieve a considerable flexibility to modulate effective permittivity and permeability from negative to zero/low index values [2,5,19,20]. Dimensional parameters are shown in Table 1. The total thickness of our designed structure is 1.07 μm , such thin metamaterials can be applied to replace some complex thick multilayer stacks or three-dimensional structure metamaterials [21,22]. The silver layer follows the Drude model:

$$\varepsilon(\omega) = 1 - \frac{\omega_p^2}{\omega^2 - i\omega\gamma_D} \quad (1)$$

Here, $\omega_p = 1.37 \times 10^{16} \text{ s}^{-1}$ is the plasma frequency, $\gamma = 9 \times 10^{13} \text{ s}^{-1}$ is the collision frequency [23].

Two distinct transmission peaks are observed at $f_1 = 90.0 \text{ THz}$ and $f_2 = 105.0 \text{ THz}$ in Fig. 1(c). To validate the structure design, we fabricate the metamaterials filter, as follows: first, two layers of silicon nitride (Si_3N_4) are deposited onto the upper and lower surfaces of silicon wafer by low pressure chemical vapor deposition, as shown in Fig. 2(a). A 1.0 μm thick layer of SU-8 is spin onto the upper surface of the silicon nitride. The SU-8 layer with composite structure of holes arrays is fabricated by optical lithography [24], as shown in Fig. 2(c). Then, two layers of silicon nitride are etched by using a reactive ion-beam etching (RIE) technology and the silicon layer is etched down by using KOH wet etching, as shown in Fig. 2(d). Finally, two layers (thick 0.035 μm) of silver are deposited by thermal evaporation onto the upper and lower surfaces of the floating hollow SU-8 layer (Fig. 2(e)). The active area of samples are around $3 \times 3 \text{ mm}^2$. The samples is placed on a metal base and characterized by a JEOL JSM-5610LV scanning electron microscope (SEM), as shown in Fig. 2(f). The measured transmission spectrum of the samples is obtained by a Bruker Optics Equinox 55 Fourier transform infrared spectrometer at normal incidence which is shown in Fig. 1(c).

3. Optical properties of the broad pass-band metamaterials filter

We define $\Delta f = f_2 - f_1$ to characterize such a unique resonant pass-bandwidth. Across the pass-band in Fig. 1(c), the average transmitted energy is 96% and the variation of transmission energy is less than 5.6%. Such an optical metamaterials filter with stable and high value of pass-band is superior to previously reported

Table 1

All dimensional parameters of the compound structure.

Parameter	p	$w1$	$w2$	$h1$	$h2$
Value (μm)	28	3.5	17	1.0	0.035

structural metamaterials [25–27]. The agreement between simulated and measured results in Fig. 1(c) verifies that our simulated results are valid. To understand the physical mechanism behind the pass-band, we retrieve the effective refractive index, permeability and permittivity by applying S parameters retrieval methods [28]. Two strong magnetic resonance modes in $\text{Re}(\mu)$ are observed and the $\text{Re}(\mu)$ increases from $\mu_{\text{eff}} = -0.09$ at 93.0 THz to $\mu_{\text{eff}} = +0.12$ at 98.1 THz, with a zero crossing at 96.1 THz. Meanwhile, two anti-resonances of $\text{Re}(\varepsilon)$ are excited by magnetic resonance modes [29], and $\text{Re}(\varepsilon)$ increases from $\varepsilon_{\text{eff}} = -0.12$ to $\varepsilon_{\text{eff}} = +0.11$. As shown in Fig. 3(a), the $\text{Re}(\mu)$ and $\text{Re}(\varepsilon)$ follow a similar slope across the same resonance frequency range which results in a well-matched impedance to free space:

$$Z_{\text{eff}} = \sqrt{\mu_{\text{eff}}/\varepsilon_{\text{eff}}} = Z_0 \quad (2)$$

Here, Z_{eff} , μ_{eff} and ε_{eff} are the real parts of the effective impedance, permeability and permittivity, respectively. A nearly constant effective impedance is observed with a small variation of 3.5%. As shown in Fig. 3(b), imaginary parts of effective parameters are minimized in the whole pass-band which results in the low absorption loss for the electromagnetic wave. These behaviors of Z_{eff} , μ_{eff} and ε_{eff} lead to n_{eff} increased from $n_{\text{eff}} = -0.11$ to $n_{\text{eff}} = 0.12$. By comparing the real part of permeability and permittivity in the pass-band, it can be found that the fabricated metamaterials filter can be modulated from a double negative material to a normal material, as shown in Fig. 3(a). Outside the pass-band, $\text{Re}(\mu)$ and $\text{Re}(\varepsilon)$ are imbalanced which leads to the real part of the effective impedance mis-matched to free space and block transmission of electromagnetic wave. At the same time, we calculate electric field distributions on the xoz plane, as shown in Fig. 4. The localized surface plasmon (LSP) mode near the lower and upper air hole edges are obviously. Moreover, the coupling and interaction of LSP modes (Fig. 4(b–d)) between the lower and upper air hole edges is observed across the pass-band. On the contrary, these coupling and interaction behaviors can't be found outside the pass-band, as shown in Fig. 4(a, e).

The influence of air nano-hole on the pass-band is studied, as shown in Fig. 5. Measured results indicate that Δf is increased and the average pass-band transmission is reduced from 96% to 90.1% with $w2$ increasing from 3.5 μm to 5.0 μm . Fig. 6 shows the effect of nano-holes on optical properties of metamaterials

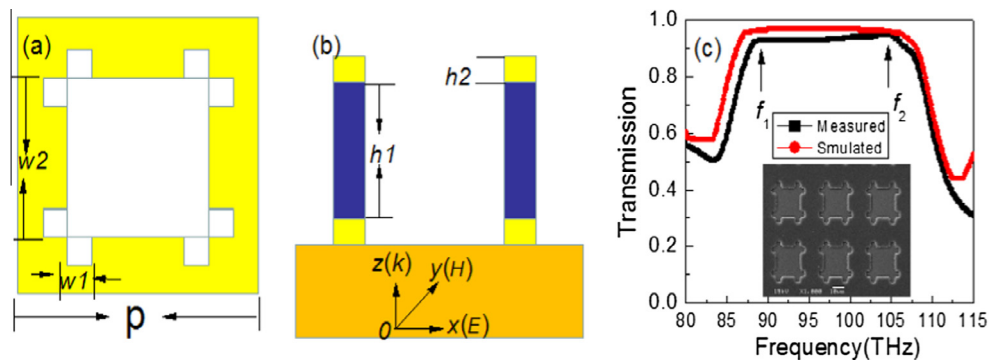


Fig. 1. (a) The top view of a unit cell; (b) the side view of a unit cell on the xoz plane. The yellow part is silver layer, the orange part is metal base of scanning electron microscopy, and the light blue part is SU-8 dielectric layer. (c) Measured (black curve) and simulated (red curve) transmission spectra of samples, the inset is the SEM of samples. (For interpretation of the references to colour in this figure legend, the reader is referred to the web version of this article.)

Download English Version:

<https://daneshyari.com/en/article/1493679>

Download Persian Version:

<https://daneshyari.com/article/1493679>

[Daneshyari.com](https://daneshyari.com)